

Coordinated Energy Flow Management in a Multi-Source Hybrid System Combining Battery Storage, Diesel, Wind, and PV

Pranati Katyal¹, Rajesh Katyal², K. Premkumar³

¹Professor, EEE, Misrimal Navajee Munoth Jain Engineering college, Thoraipakkam, Chennai.

²Director General, National institute of Wind Energy, Chennai.

³Associate Professor, Department of EEE, Rajalakshmi Engineering College, Chennai

E-mail: pranati.kat@gmail.com¹, Katyal.niwe@nic.in², premkumar.k@rajalakshmi.edu.in³

Article Received: 25 Sep 2025

Article Accepted: 13 Nov 2025

Article Published: 17 Nov 2025

Citation

Pranati Katyal, Rajesh Katyal, K. Premkumar (2025), "Coordinated Energy Flow Management in a Multi-Source Hybrid System Combining Battery Storage, Diesel, Wind, and PV", Journal of Next Generation Technology, 5(6), pp. 70-90, Nov 2025.

Abstract

This paper investigates an integrated energy management context for hybrid power system comprising PV arrays, wind energy conversion systems, a diesel generator, and battery energy storage, implemented in MATLAB/Simulink. The central objective is to regulate power sharing among the multiple sources to guarantee reliability and operational efficiency. The fusion of intermittent renewable resources with conventional diesel units introduces significant challenges in maintaining supply–demand equilibrium, especially under fluctuating solar irradiance, wind velocity, and load variations. The proposed energy management system prioritizes renewable penetration by maximizing PV and wind utilization through MPPT, while employing the battery to buffer mismatches between generation and demand. Consequently, the diesel generator operates primarily as a backup, thereby reducing fuel absorption and conservatory gas emissions. The EMS employs a dynamic control strategy based on real-time measurements, ensuring optimal dispatch of resources and stable DC-link voltage. Simulation studies confirm that the hybrid EMS enhances fuel savings, improves voltage regulation, and strengthens system resilience against uncertainties in weather and load.

Keywords: Hybrid Energy System Energy Management System, Photovoltaic, Wind Energy Conversion System, Diesel Generator, Maximum Power Point Tracking, Renewable–Diesel Integration, Microgrid Stability.

Nomenclature

Abbrev.	Meaning
HRES	Hybrid Renewable Energy System
RES	Renewable Energy System
HPP	Hybrid Power Plant
BESS	Battery Energy Storage System
PV	Photovoltaic
WT	Wind Turbine

DG	Diesel Generator
BESS	Battery Energy Storage System
EMS	Energy Management System
MPPT	Maximum Power Point Tracking
MPP	Maximum Power Point
P&O	Perturb & Observe
NMPC	Nonlinear Model Predictive Control
MPC	Model Predictive Control
MILP	Mixed-Integer Linear Programming
SDDP	Stochastic Dual Dynamic Programming
FLC	Fuzzy Logic Control
IPMC	Intelligent Power Management Control
GA	Genetic Algorithm
PSO	Particle Swarm Optimization
GWO	Grey Wolf Optimizer
GWCSO	Grey Wolf–Cuckoo Search Optimization
CSO	Cuckoo Search Optimization
ALO	Ant Lion Optimizer
DFIG	Doubly-Fed Induction Generator
PMSG	Permanent Magnet Synchronous Generator
HIL	Hardware-in-the-Loop
PCC	Point of Common Coupling
LCOE	Levelized Cost of Energy
SOC	State of Charge
WECS	Wind Energy Conversion System
DG	Diesel Generator
GHG	Greenhouse Gas
HPP	Hybrid Power Plant
DC	Direct Current
THD	Total Harmonic Distortion
PV	Photovoltaic

I. Introduction

The incorporation of RES into contemporary power systems has enhanced due to rising request for clean and dependable electricity on a wide-reaching scale. The ability of PV modules and wind turbines to lower carbon emissions and reliance on fossil fuels is well known. However, maintaining a steady power supply is made extremely difficult by their erratic and fluctuating nature, particularly in remote or stand-alone applications. Hybrid systems that combine traditional diesel generators, RES, and BESS have become a viable way to address these problems. By using diesel backup and storage support, these systems provide supply continuity while leveraging the complimentary behavior of RES. The addition of RES into hybrid systems has been a growing research focus,

particularly due to the inherent variability and intermittency of PV and wind power. A study in [1] emphasized that while renewable sources introduce uncertainties in generation, these limitations can be mitigated by integrating multiple sources and storage units. However, such diversification increases the system's cost and complexity, thereby making optimization and EMS indispensable. The work highlighted that proper EMS ensures reduced energy costs, improved efficiency, and continuous load supply. In [2], the microgrid operation and an EMS based on NMPC were analysed to address the imbalance between generation and demand. Their approach prioritized intelligent scheduling of loads, management of battery charge–discharge cycles, and ensured microgrid resilience even during controller failures. The results demonstrated stable voltage and frequency regulation, proving the robustness of the NMPC-based EMS.

The need for integrated approaches combining EMS with RES was further reinforced in [3]. The study reviewed EMS and technologies, showing that coordinated frameworks significantly reduce GHG and energy consumption. The findings underscore that hybrid strategies not only enhance sustainability but also yield considerable economic benefits.

HRES are particularly beneficial for rural and remote electrification. Reference [4] discussed the importance of optimal sizing, intelligent energy storage, and advanced control approaches to reduce grid dependency. GA and solar PV forecasting were highlighted as essential tools for system optimization and planning. Similarly, [5] extended this by presenting applications of evolutionary and nature-inspired procedures like PSO and GA for efficient control and power management. Their analysis showed that hybrid systems backed with intelligent EMS outperform single-source systems in terms of reliability and power quality. The feasibility of dispatch strategies in hybrid systems was investigated in [6]. The study compared load-following, cycle charging, and combined dispatch approaches using HOMER software for a PV–diesel–battery configuration. The combined dispatch strategy provided the most promising results, achieving lower cost, reduced and significant cuts of CO₂ emissions, confirming its economic and environmental advantages. Advanced intelligent control methods were also explored in [7], where an IPMC framework using fuzzy logic was proposed for autonomous hybrid systems. This adaptive system dynamically optimized power flows under varying weather and heavy load conditions. Simulation results validated that the fuzzy logic-based controller enhanced availability, extended the lifespan of components, and maintained balanced operation.

In [8], MPC was applied for dispatch optimization in a hybrid microgrid. The closed-loop MPC model demonstrated strong robustness against uncertainties and disturbances compared to the open-loop model. Seasonal variations were also captured, showing higher diesel consumption during winter. The study highlighted MPC as a promising tool for predictive and adaptive EMS design. The techno-economic optimization of PV–battery–diesel systems was studied in [9], where PSO was employed for optimal sizing under cost and emission constraints. The framework evaluated multiple scenarios, including different battery depths of discharge. Case study results confirmed that the hybrid system offered lower overall cost and shorter payback compared to DG-only or PV–battery-only systems, emphasizing the economic viability of hybridization. In [10], a hybrid MG composed of PV, wind, biomass gasifiers, DGs, and batteries was developed for Basra city in Iraq. For optimal sizing, a novel hybrid GWCSO algorithm was introduced and benchmarked against PSO, GA, GWO, CSO, and ALO. Results showed that GWCSO achieved superior robustness and yielded the lowest LCOE of 0.1192 \$/kWh, demonstrating its effectiveness in minimizing system cost and emissions. Experimental validation of hybrid systems was highlighted in [11], where standalone system was constructed and tested. The setup included a 1 kW PMSG, charge controller, inverter, diesel unit, and load prototype. The study examined system performance under three operational scenarios varying wind speed and battery state of charge. Results confirmed reliable operation across all modes, with real-time monitoring using data loggers and sensors improving supervision and fault intervention capabilities. In [12], a BEMS for microgrids combining PV and diesel sources was proposed. The

approach emphasized concurrent control of multiple batteries with differing characteristics while minimizing diesel generator usage. By intelligently managing charge–discharge cycles, the system not only reduced PV fluctuations but also extended battery life. Case studies using real-world data validated the method, confirming reductions in DG runtime and smoother renewable integration.

A supervisory control technique of hybrid system with battery assistance was provided in [13]. The system used FLC to dynamically distribute power flows according to changes in the weather. FLC is a viable option for hybrid EMS as it was implemented in MATLAB for the Bejaia region of Algeria. The findings showed efficient and straightforward decision-making for hybrid power balancing. Optimization-oriented MPPT approaches were investigated in [14], where a DC microgrid combining PV, wind, diesel, and batteries was studied. The proposed GWO-based MPPT method dynamically adjusted converter duty cycles, outperforming conventional techniques in response time and oscillation suppression. Simulation and experimental findings showed enhanced bus voltage stability and adaptability under fast-changing irradiance and load conditions.

A communication-free EMS for hybrid PV–battery–diesel systems was introduced in [15]. The method avoided long control cables by using frequency-shift signaling: battery inverters increased grid frequency to signal PV inverters to curtail power when batteries were full. This simplified the system design while ensuring battery protection and optimized diesel operation. Both simulation and experimental validation confirmed the strategy’s effectiveness in improving reliability and reducing costs. [16] focused on techno-economic evaluations, evaluating several hybrid configurations in Tamil Nadu, India. Across several sites, the hybrid combination was determined. Thoothukudi had the lowest power costs, while diesel-only systems had the lowest costs (\$1.88/kWh). The results also showed notable decreases in CO₂ emissions, demonstrating the benefits of hybridization for the environment and the economy.

In [17], coordinated control of hybrid microgrids was examined. The study implemented PO and Optimal Power Controlling MPPT methods to improve resource utilization. A centralized supervisory control ensured dynamic load balancing and stability. Findings showed that real-time HIL models could effectively guide microgrid design, with future work aimed at refining accuracy and validating the approach in practical deployments. In [18]-[20] developed a real-time EMS framework for HPPs integrating PV, batteries, diesel, and pumped hydro storage. Two optimization methods MILP and SDDP were applied. The SDDP approach consistently achieved lower costs and CO₂ emissions, with daily operation costs of \$180 compared to \$219.8 for MILP. The results highlighted the superiority of SDDP in managing uncertainties, optimizing BESS operation, and reducing emissions, thus offering a practical roadmap for hybrid plant operation.

A. Background of the study

The hybrid PV–wind–diesel–battery systems face

- (1) uncoordinated energy dispatch leading to power imbalance and inefficient renewable utilization,
- (2) limited adaptability of existing EMS under fluctuating irradiance, wind, and load conditions, and
- (3) inefficient diesel fuel and battery management due to static control logic. Hence, this study formulates an adaptive EMS to ensure conflict-free power sharing, optimal SoC regulation, and reduced fuel consumption for enhanced hybrid system efficiency.

Efficient operation of hybrid systems requires an effective energy management strategy capable of coordinating multiple sources under dynamic load and weather conditions. By employing advanced methods, the system can maximize renewable contribution while minimizing fuel consumption and emissions from the diesel generator. The battery serves as a critical element to smooth fluctuations and balance short-term mismatches between demand and generation. This study

focuses on highlighting how the proposed energy management framework enhances stability, fuel savings, and overall system reliability.

The aim is to achieve conflict-free power sharing, maintain DC-link stability, and minimize diesel fuel consumption while sustaining power quality under varying irradiance and load conditions.

II. Literature Review

The structure of an HRES that combines PV modules, a wind power system, a (DG), and a BESS is depicted in the schematic in Figure 1. The design guarantees a steady supply to many AC loads across a range of demand and weather scenarios. Through a DC connection and an inverter, the DC power produced by the PV array is connected to the common AC bus. Direct coupling between the wind turbines and DG and the AC bus provides active power to satisfy load demands. According to power balance circumstances, a bidirectional converter that links the DC connection to the BESS permits both charging as well as discharge activities. This structure enables flexible utilization of renewable resources while minimizing DG operation. The battery compensates for intermitencies, maintains power quality, and provides backup during contingencies.

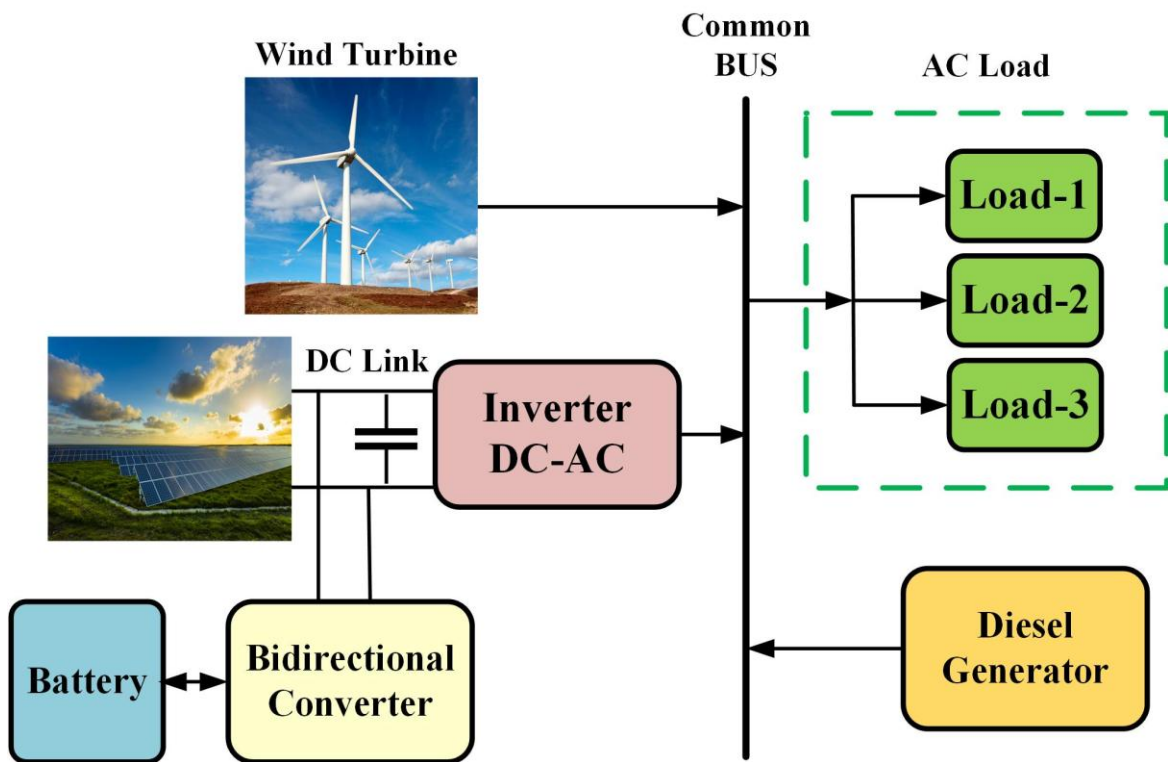


Figure.1 Proposed System Architecture

A. PV Modelling

The photovoltaic PV system is generally represented by an equivalent electrical circuit represented in Figure 2. Among several available models, single-diode model is commonly adopted due to its balance between computational efficiency and physical accuracy. It is sufficient to predict system behavior under varying irradiance and temperature conditions without requiring extensive parameterization. In this model, the total PV current is expressed as,

$$I_{PV} = I_{ph} - I_d - I_{Rsh} \quad (1)$$

Where, I_{ph} represents the photocurrent generated when photons strike the semiconductor surface, proportional to solar irradiance and slightly dependent on temperature. I_d denotes the diode current,

arising from the intrinsic p–n junction of the solar cell. I_{Rsh} accounts for leakage current through the shunt resistance, which becomes significant when shunt losses are high. Expanding this using the diode law, the current equation becomes,

$$I = I_{sc} - I_0 \left(e^{\frac{q(V+IR_s)}{N_s \alpha k T}} - 1 \right) - \frac{V+IR_s}{R_{sh}} \quad (2)$$

This nonlinear relationship indicates that PV output is highly sensitive to irradiance and temperature changes, hence the requirement for control mechanisms to maximize efficiency.

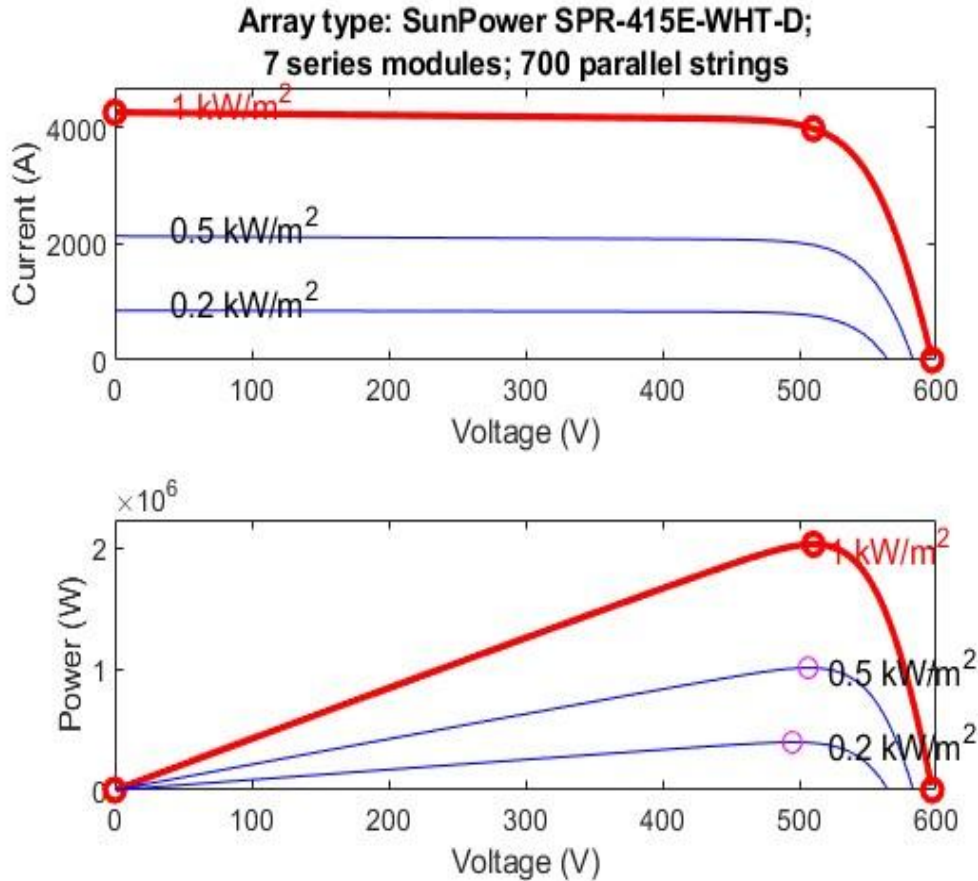


Figure 2. Characteristics of PV

MPPT using PO

Step 1 : A small perturbation ΔV is introduced to the PV operating voltage.

Step 2 : The resulting change in output power ΔP is measured.

Step 3 : If $\Delta P > 0$, this implies the perturbation has moved the operating point closer to the MPP, so the algorithm continues perturbing in the same direction.

Step 4 : If $\Delta P < 0$, the perturbation has shifted the operating point away from the MPP, and the direction of perturbation is reversed.

Step 5 : Steps 1–4 are repeated continuously, ensuring convergence toward the MPP.

Mathematically, the decision logic can be expressed as,

$$\text{If } \frac{\Delta P}{\Delta V} > 0 \rightarrow V_{new} = V_{old} + \Delta V \quad (3)$$

$$\text{If } \frac{\Delta P}{\Delta V} < 0 \rightarrow V_{new} = V_{old} - \Delta V \quad (4)$$

Where,

$$\Delta P = P(k) - P(k - 1) \quad (5)$$

$$\Delta V = V(k) - V(k - 1) \quad (6)$$

B. Wind Model

The wind turbine converts wind energy into mechanical energy, which is subsequently transformed into electrical power through the use of DFIG. This configuration is widely preferred for wind energy conversion due to its variable-speed operation, high efficiency, and ability to regulate both active and reactive power independently. A 1.5 MW WECS is used in this study. The power extracted from the wind is governed by the aerodynamic equation,

$$P_w = \frac{1}{2} C_p(\lambda, \beta) \rho A V_w^3 \quad (7)$$

The coefficient C_p represents how effectively the turbine captures wind energy, with a theoretical upper limit known as Betz's limit (0.593). The "tip-speed ratio λ " is defined as the ratio, and the pitch angle β controls the aerodynamic performance. The corresponding aerodynamic torque applied to the turbine shaft is expressed as,

$$T_w = \frac{P_w}{\omega_r} \quad (8)$$

Here ω_r is "rotor angular velocity". Thus, torque output depends on "wind speed, rotor size" and rotational speed, emphasizing the importance of optimal control strategies for efficiency. The DFIG operates with "stator windings directly connected to the grid and rotor windings interfaced via back-to-back converters", enabling bidirectional power flow. The developed electromagnetic torque is given by.

$$T_{em} = \frac{3}{2} P [(L_{ds} - L_{qs}) I_{ds} I_{qs} + \phi_f I_{qs}] \quad (9)$$

Here, R_s is "stator resistance" L_{ds} , L_{qs} are "dq-axis inductances" I_{ds} , I_{qs} are "dq-axis stator currents" and ϕ_f is "rotor flux linkage produced by permanent magnets". where P denotes the number of pole pairs. This equation highlights that torque is influenced both by current components and by rotor flux linkage, allowing precise control of active and reactive power through vector control strategies.

C. Diesel Generator

The DG complements renewable sources during peak demand or low resource availability. The generator model includes speed control, actuator dynamics, and synchronous generator behavior. The mechanical–electrical torque balance is,

$$T_d - T_{em} = J \frac{d\Omega_m}{dt} \quad (10)$$

where T_d is "mechanical torque" T_{em} "electromagnetic torque" J "moment of inertia" and Ω_m angular speed. The fuel consumption characteristic is nonlinear and approximated as:

$$F_{DG} = a P_{DG}^2 + b P_{DG} + c \quad (11)$$

with coefficients a, b, c obtained from empirical testing. Control loops (droop and PI-based governor) ensure frequency and voltage regulation.

D. Model of Battery

The BESS plays a pivotal role in hybrid energy systems by providing energy balancing, load-levelling, and backup support. This configuration defines a Li-Ion battery model with a nominal voltage of 300 V, a rated capacity of 6500 Ah, and an initial state of charge set at 75%, while ignoring temperature and aging effects. This capability makes BESS essential for mitigating renewable intermittency, enhancing system reliability. The fundamental equation of battery is given as,

$$V_{bat} = E_{bat} \pm R_{bat} I_{bat} \quad (12)$$

The open-circuit voltage E_{bat} and overall performance strongly depend on the SoC, which is dynamically updated as,

$$SOC(t + 1) = SOC(t) + \frac{\eta_c P_{ch}(t)\Delta t}{C_{bat}V_{nom}} - \frac{P_{dis}(t)\Delta t}{\eta_d C_{bat}V_{nom}} \quad (13)$$

where P_{ch} and P_{dis} are charging and discharging powers, η_c and η_d are efficiencies, and C_{bat} is the nominal capacity. Maintaining the SoC within safe bounds (typically 20–90%) prevents overcharging, deep discharging, and premature battery degradation.

III. Proposed Control Techniques

The selection of appropriate control techniques for hybrid energy systems is influenced by several critical issues: (i) nonlinearity of renewable sources and converter dynamics; (ii) variability in solar irradiance and wind speed; (iii) the need for fast response during load transients; (iv) battery SoC and converter limitations; and (v) trade-offs between control complexity and computational burden. Hence, a combination of classical PI regulation and MPPT-based adaptive control was selected for stability and real-time implementation.

A. PV Inverter control

The block diagram provided Figure 3 shows the photovoltaic (PV) inverter's control method, which uses feedforward decoupling compensation, PI regulation, and dq-axis control to provide steady grid integration and maximum power extract from the PV array. The whole control system eliminates unwanted harmonics in the injected current, coordinates inverter operations with the grid, and maintains the DC-link voltage.

a. *abc–dq₀ Transformation Block*

It converts “three-phase grid voltage (V_g) and current (I_g)” signals from the stationary reference frame into their equivalent rotating reference frame components along d and q axes. This transformation simplifies the control design by separating the active and reactive power components. The d -axis current I_{dact} corresponds to the control of active power flow, whereas the q -axis current I_{qact} controls reactive power exchange. These transformed quantities form the essential feedback inputs for current regulation in the inverter control loop.

b. *Reference Current Generation*

The reference current generation and comparison stage involves comparing I_{dact} , I_{qact} with their respective reference values I_{dref} , and I_{qref} . These reference currents are derived from the DC-link voltage controller, ensuring that the inverter injects the desired amount of real and reactive power into the grid. The resulting current error signals represent the instantaneous deviation between actual and desired current magnitudes. These error signals are after managed by proportional–integral (PI) controllers to maintain accurate current tracking and eliminate steady-state errors.

c. *PI Controllers*

The key regulating component of the control system is the PI controller block. It generates the matching voltage-controlled outputs V_d , V_q after receiving the error data from the d and q axes. Although the integral term corrects for steady-state inaccuracy, the proportional term guarantees a quick dynamic reaction. In order to preserve the intended current and voltage profiles, they work together to modify the inverter output. As a result, the controller ensures that the inverter efficiently synchronizes with the grid and provides distortion-free, seamless power transmission in both constant and transient scenarios.

d. *Feedforward Decoupling Control*

The feedforward decoupling control block is implemented to mitigate the inherent coupling between the d and q current components caused by cross terms in the voltage equations of the inverter. Without decoupling, a change in one current component would inadvertently affect the other, leading to sluggish response and instability. The feedforward control compensates for these

coupling effects by injecting corrective voltage terms into the control loop. As a result, the d - and q -axis dynamics become independent, enhancing control accuracy and system stability during dynamic grid or load variations.

e. $dq0$ - abc Inverse Transformation

The inverse $dq0$ - abc transformation block converts the regulated d - and q -axis voltage components V_d, V_q back to three-phase stationary reference frame signals V_a, V_b, V_c . This conversion is necessary for generating the three-phase sinusoidal voltage references required for the pulse-width modulation (PWM) process.

f. PWM Generator

The PWM generator block receives 3-phase voltage references V_a, V_b, V_c . and compares them to high-frequency triangular carrier waveform to generate gating pulses. The resultant PWM indications determine on-off states of the inverter switches, thereby controlling output voltage. This modulation process allows the inverter to inject current into the grid with precise control over magnitude and phase, ensuring efficient with grid values.

g. PO MPPT

The P&O MPPT block continuously monitors the instantaneous PV array voltage V_{pv} and current I_{pv} to extract maximum power under varying irradiance and temperature conditions. The program examines how the power output changes in response to perturbations in the operating voltage. The operational voltage is changed in the exact same direction as the power increase, or in the opposite direction of the perturbation. This repeated procedure ensures optimal energy use of the solar array by operating the PV system at its highest power point.

h. Voltage Regulator

The **voltage regulator block** maintains $V_{dc\ link}$ at a constant reference level by regulating the current reference signals fed to the inverter control loop. It does a comparison between the reference voltage derived by the MPPT controller and the observed DC-link voltage. A controller known as PI within the voltage regulator processes the difference between the two to produce a reference d-axis current I_{dref} , that controls the flow of active power. In order to preserve unity power factor operation, the q-axis current standard I_{qref} is usually set to zero. This keeps the voltage across the DC connection stable and guarantees that the inverter only sends actual electricity to the grid.

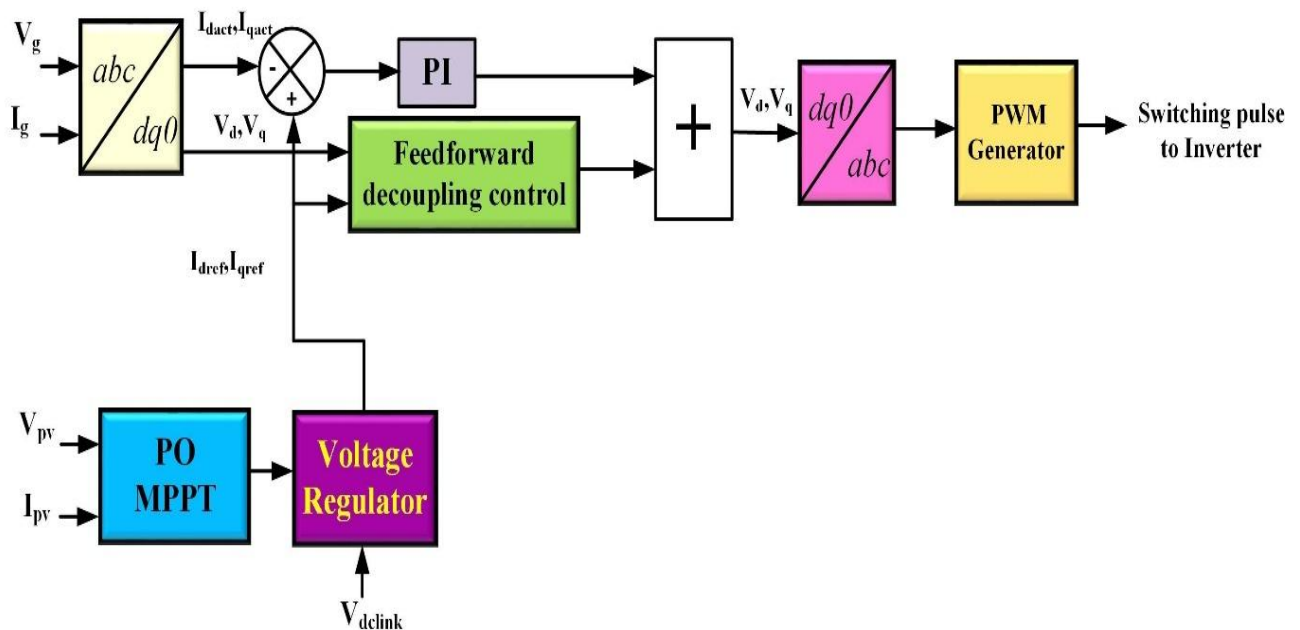


Figure 3. PV Inverter control

B. Energy Management Control

The control framework illustrated in Figure 4. shows the battery's bidirectional power management under two operational modes.

Mode-1: Load-Reference Based Control

- In this mode, the load power (P_{load}) is continuously monitored and compared with a predefined reference power (P_{ref}).
- The resulting error signal determines the reference current (I_{ref}) required from the battery.
- If the load demand exceeds the renewable generation, the battery discharges (negative current), whereas when the load demand is low, it switches to charging mode (positive current).
- This ensures continuous and balanced power delivery to the load under varying demand conditions.

Mode-2: PV-Reference Based Control

- In this mode, the input current (I_{pv}) is compared with a predefined reference value to generate another reference current (I_{ref}).
- When PV generation exceeds the load requirement, the battery absorbs excess energy (charging mode).
- Conversely, during reduced irradiance, the battery releases stored energy (discharging mode) to maintain DC-link voltage stability and support the load.

a. Mode Selector

- The Mode Selector block serves as the decision-making element that switches between Mode-1 and Mode-2 based on system operating conditions (e.g., load variation or irradiance level).
- It selects the appropriate I_{ref} signal corresponding to either load-based or PV-based control and forwards it to the next stage.
- This hierarchical control prevents energy flow conflicts and ensures that the battery acts as a flexible buffer, maintaining a stable power balance across the DC-link.

b. PI Controller

- The selected reference current (I_{ref}) is related with measured battery current (I_{bat}), producing a current error signal.
- A proportional-integral (PI) controller processes this mistake by controlling the duty cycle of the converter in order to reduce steady-state error and preserve seamless charge-discharge transitions.
- The PI output provides a control signal corresponding to the required converter switching behavior.

c. PWM Generator

The Pulse Width Modulation (PWM) generator receives the PI controller's output and generates the switching pulses required to regulate the bidirectional DC–DC converter. These PWM signals determine whether the converter runs in boost mode (battery discharging) or buck mode (battery charging). This guarantees precise and instantaneous regulation of the energy transfer among the PV array, batteries, and load.

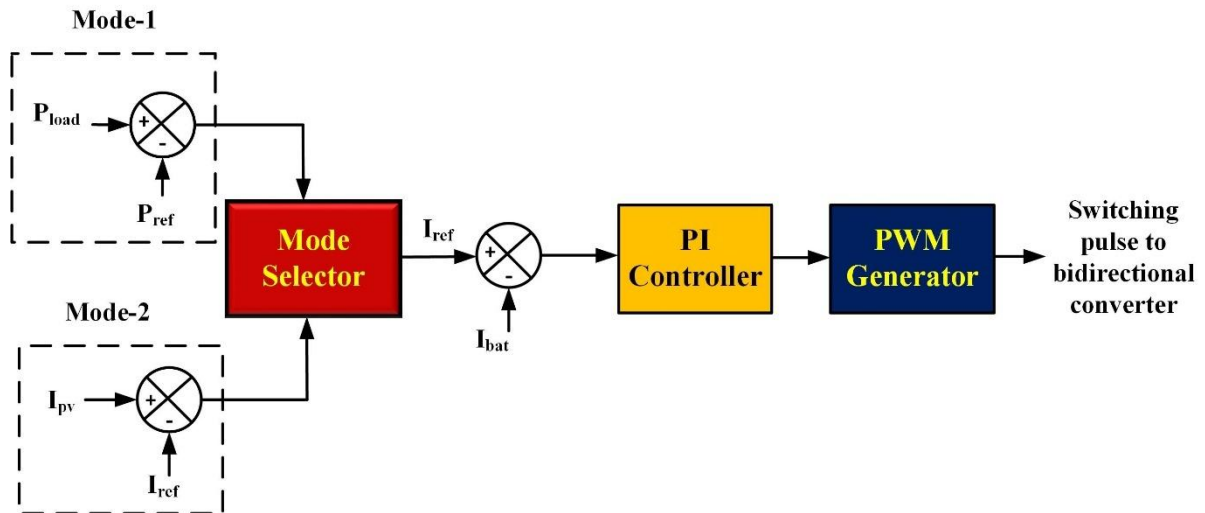


Figure 4. Energy Management Mode selection control

IV. Results And Discussions

A. Mode-1 (Varying Irradiance Condition)

In this mode, the system behavior is governed by fluctuations in solar irradiance. The PV current is measured and scaled, then compared with a reference to determine battery operation. When the irradiance increase, PV array generates excess control beyond load requirement, and battery enters charging mode to store the surplus energy. Conversely, during low irradiance conditions, when PV output falls short, the battery automatically shifts into discharging mode to supply the deficit power and maintain system stability. The irradiance profile is varied over time to simulate realistic sunlight changes.

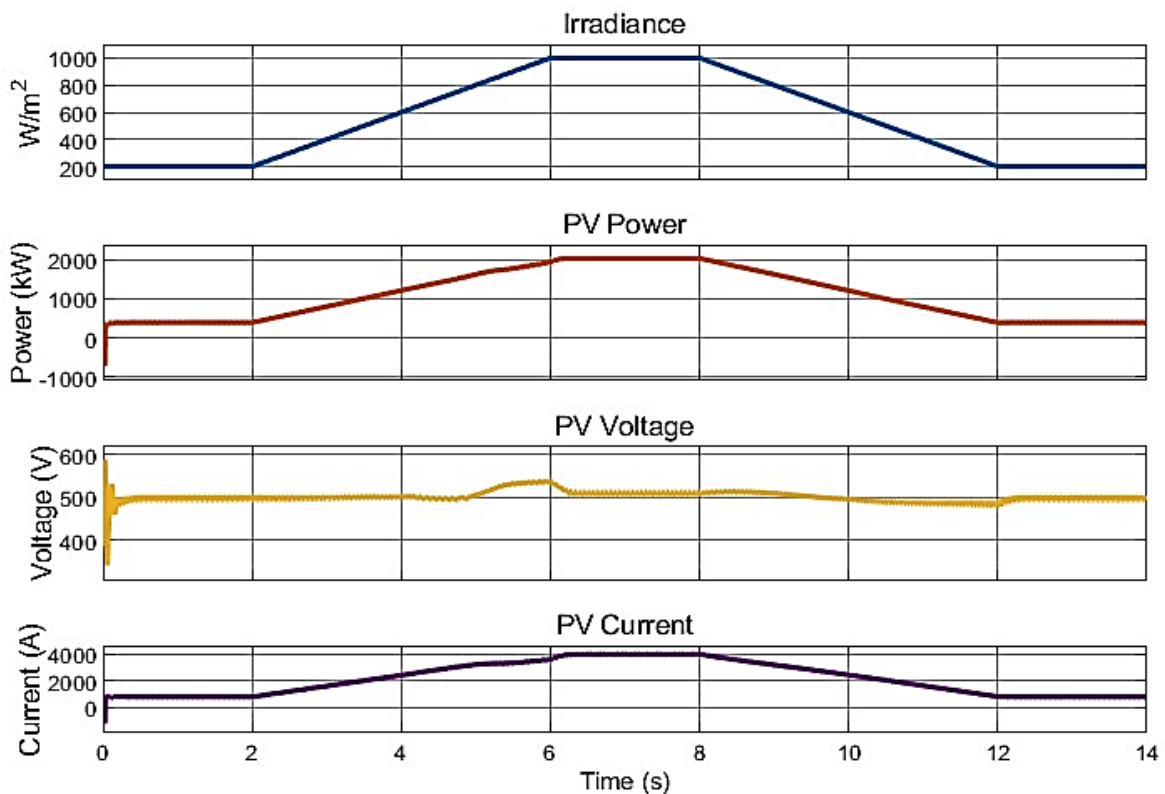


Figure 5. PV Parameters at Mode-1

The irradiance upsurges gradually from 100 to 1000 W/m², leading to a proportional rise in PV output power from about 200 kW to 1800 kW. The PV voltage remains fairly stable around 500–600 V, showing that the voltage regulator and MPPT maintain bus stability. The PV current shows significant variation, peaking at nearly 4000 A under maximum irradiance. These results confirm the successful operation of the PO MPPT procedure in extracting maximum power under varying conditions. The effective control ensures that the PV system responds dynamically to solar fluctuations without destabilizing the DC link. The Figure 5, 6, 7, 8, 9 and 10 shows the PV, wind, battery, DG, load and DC link voltage parameters at mode I respectively.

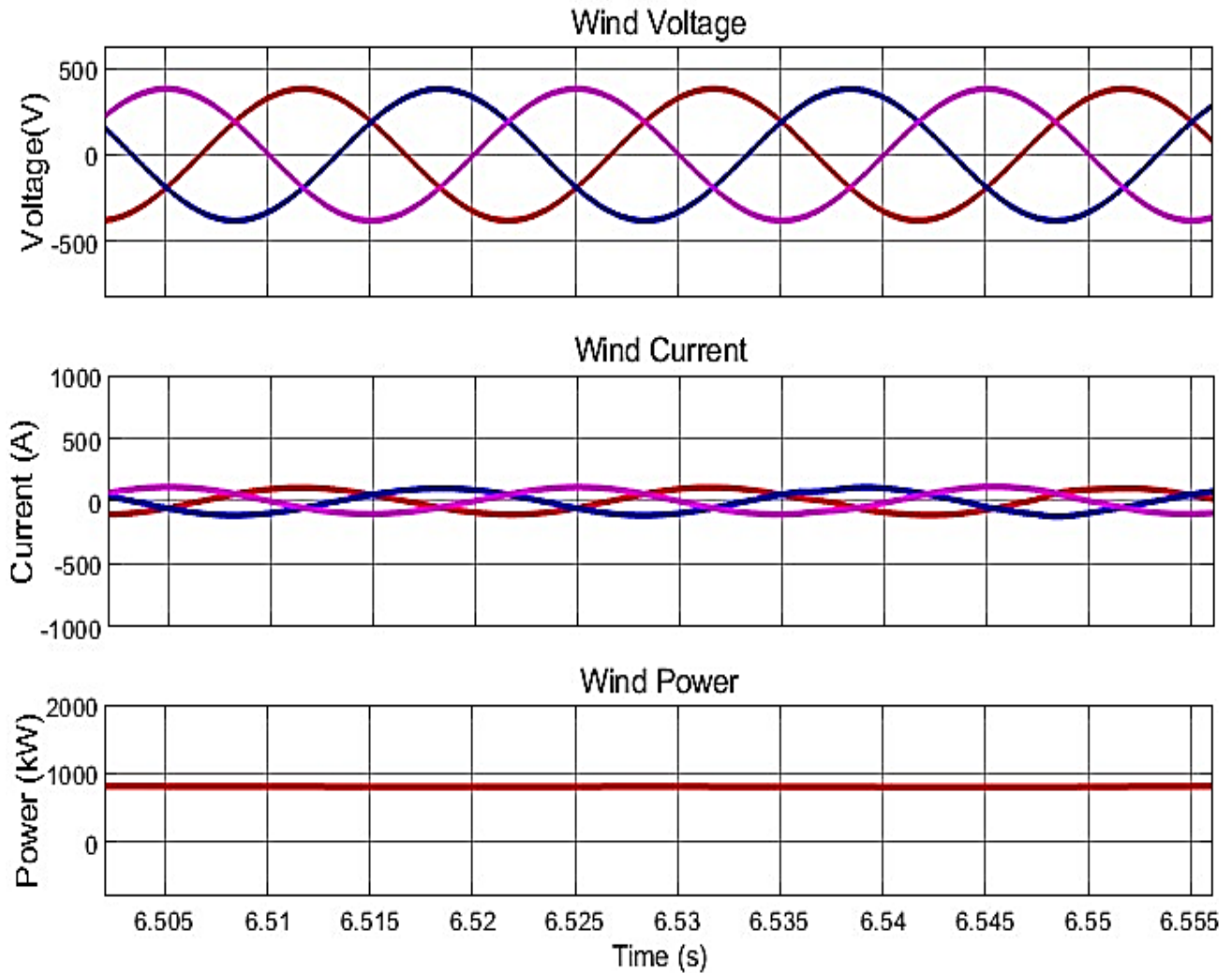


Figure 6. Wind parameters at Mode-1

The wind turbine delivers balanced three-phase sinusoidal voltages of approximately 500 V. The generated power is steady near 800 kW, demonstrating that the wind subsystem provides a stable supply independent of solar irradiance variations. The sinusoidal waveforms confirm effective dq-axis vector control and minimal harmonic distortion in the wind generator output.

The battery SoC decreases slightly from 75% to 74.98%, indicating active charge–discharge cycles during irradiance variations. Current swings between +1500 A (charging) and –500 A (discharging), while terminal voltage stabilizes in the range of 302–304 V. Battery power varies between +400 kW supply and –200 kW absorption, showing its dual role as source and sink. These dynamics highlight the BESS function in smoothing PV fluctuations and maintaining load balance.

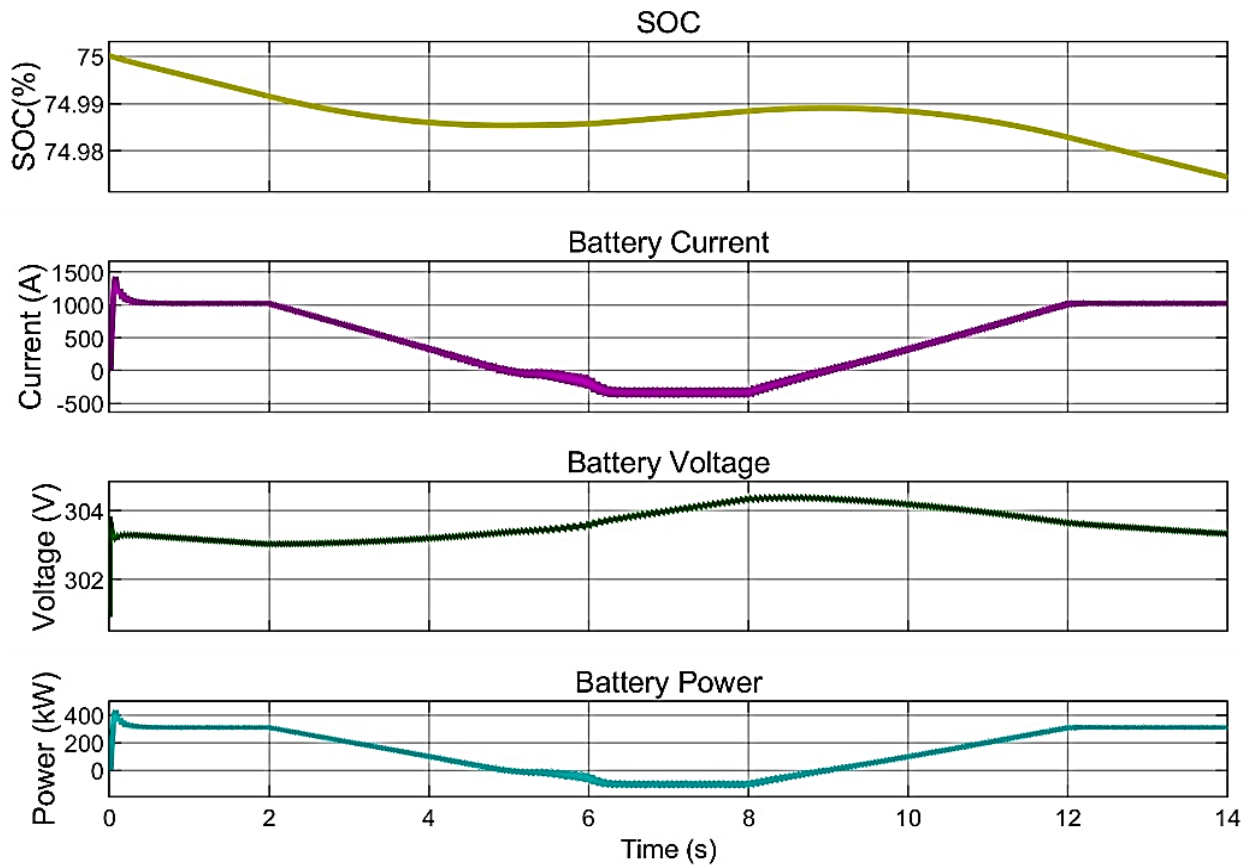


Figure 7. Battery parameters at Mode-1

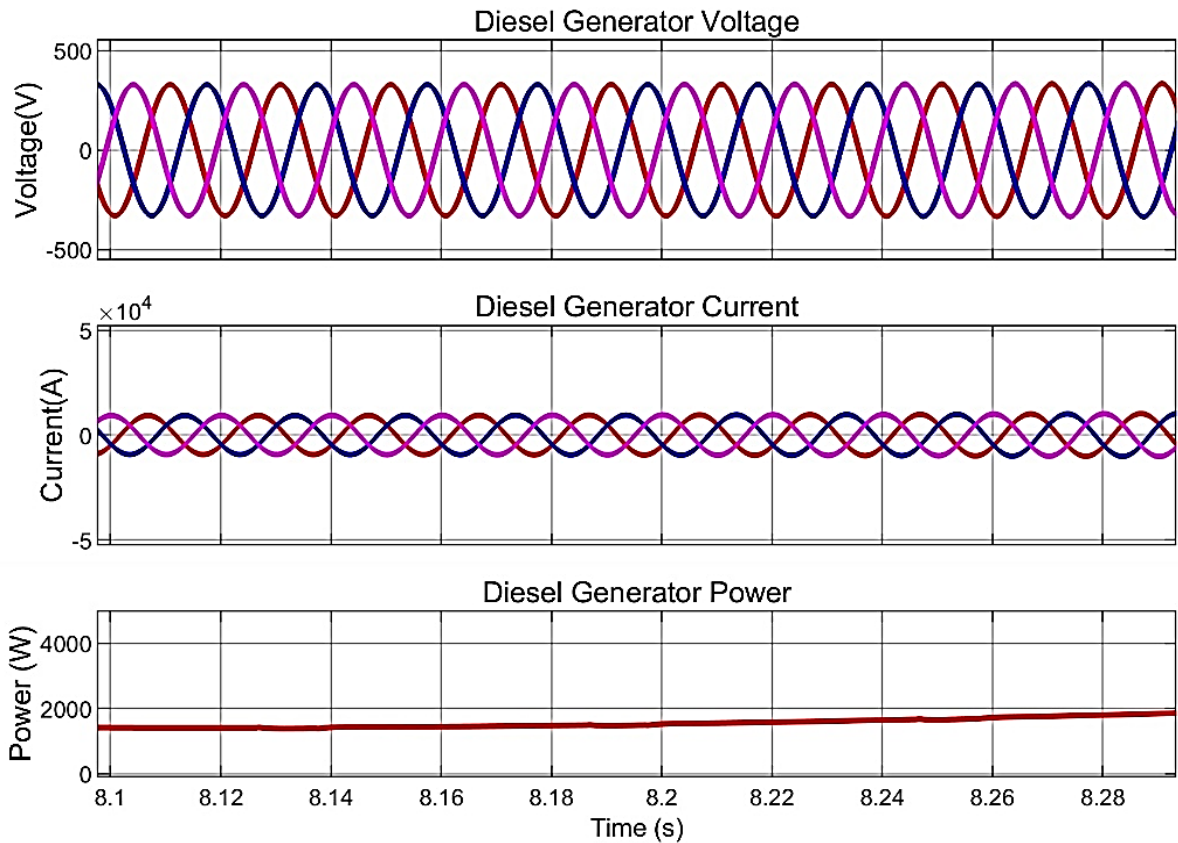


Figure 8. DG parameters at Mode-1

Figure 8 illustrates the performance of the diesel generator during varying irradiance conditions. The voltage and current waveforms remain sinusoidal and balanced, confirming proper synchronization and stable operation of the generator. The power curve shows a steady output around 2000 W, indicating that the diesel generator effectively compensates for the deficit in renewable generation when solar or wind power decreases. This demonstrates the reliability of the DG as a backup source in maintaining system stability and ensuring continuous power supply during transient variations in renewable inputs.

The DG maintains sinusoidal voltages of about 500 V and high currents, corresponding to a steady power output around 2000 kW. The near-constant power level proves that the DG operates as a stabilizing support during irradiance dips. Its contribution compensates for renewable shortfalls, thereby preventing power deficits.

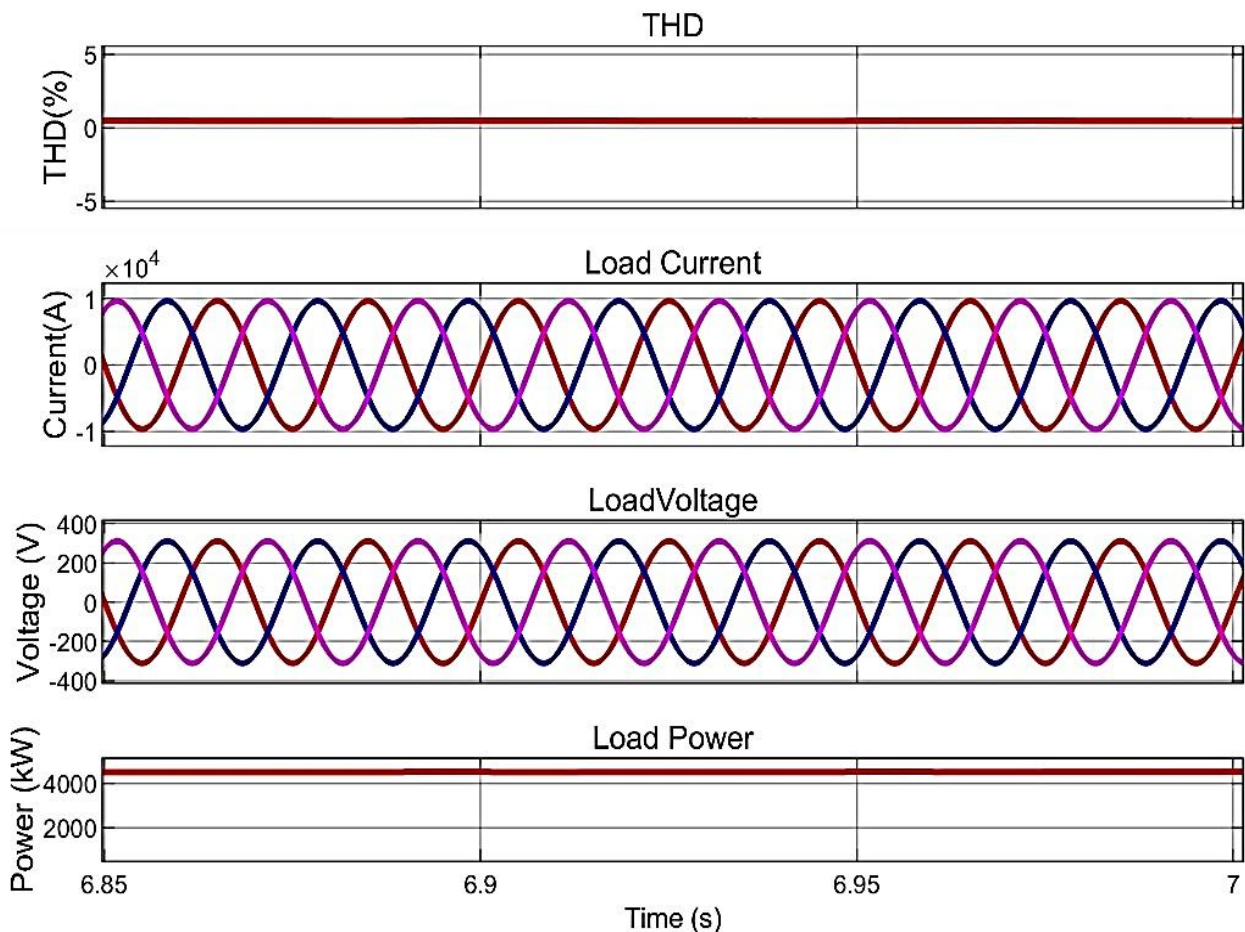


Figure 9. Load parameters at Mode-1

The load receives sinusoidal currents and voltages with consistent power around 4000 kW. Importantly, the THD remains minimal, confirming high-quality power delivery. The inverter control ensures that harmonic content is minimized despite fluctuations in renewable generation. Voltage and current profiles show no distortion, proving excellent dynamic regulation.

The DC-link voltage remains tightly regulated near 500 V, with only minor transients around 6 s and 12 s, when irradiance changes occur. The system quickly restores voltage to its nominal value, showing the robustness of the control loop. Stable DC link voltage is critical for proper inverter operation and grid synchronization. This confirms that the coordinated PV–Battery control effectively mitigates fluctuations.

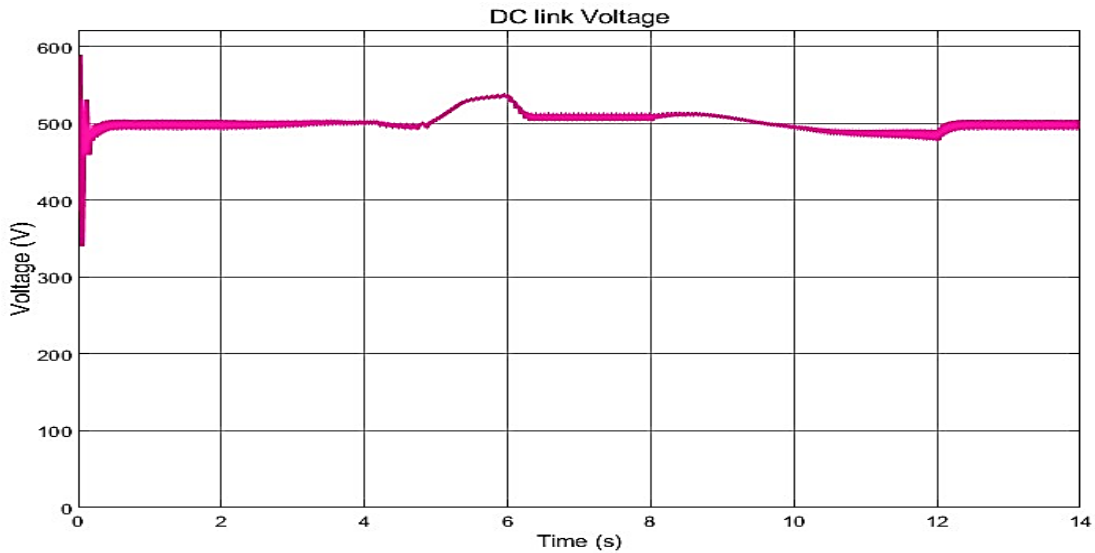


Figure 10. DC link voltage at Mode-1

B. Mode- 2 (Varying Load Condition)

In this mode, the system focuses on handling variations in load demand while maintaining constant irradiance. The load power is measured and converted into current, which is compared against a reference to decide the battery's role. When load demand is high, the battery supports the system by discharging and supplying additional power. On the other hand, during low load demand, the battery switches to charging mode, storing the surplus power produced by the PV system. This ensures balanced energy management between generation and consumption.

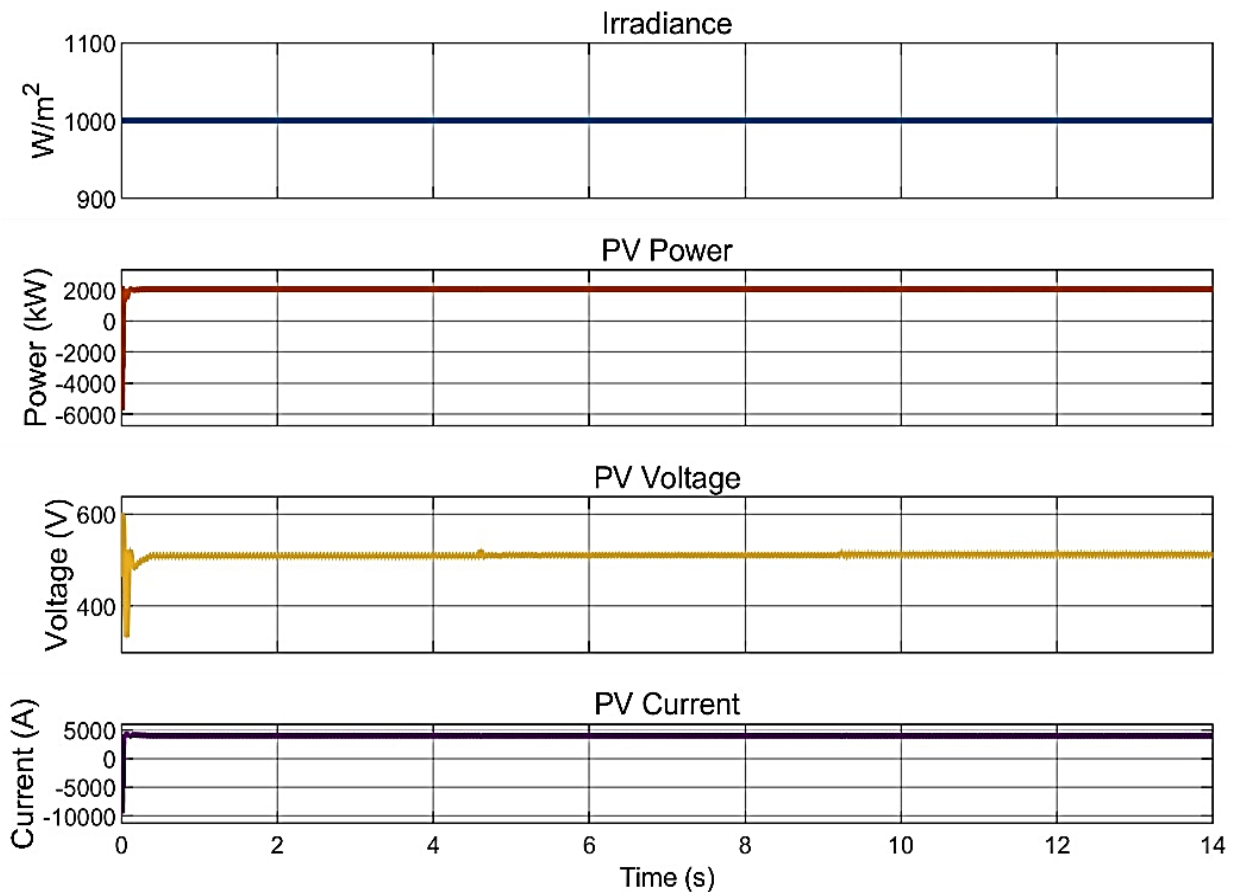


Figure 11. PV Parameters at Mode-2

The mode is activated through step signals are used to vary the load dynamically, with circuit breakers switching additional loads ON and OFF at specified times. These changes alter the load profile, and the corresponding battery reference current is generated accordingly. The PI controller processes this reference to regulate the converter duty cycle, ensuring smooth transition between charging and discharging states. This mode validates the system's ability to maintain reliable power flow under sudden changes in load demand. The Figure 11, 12, 13, 14, 15 and 16 shows the PV, wind, battery, DG, load and DC link voltage parameters at mode I respectively.

As shown in Figure 11, the irradiance remains constant at 1000 W/m^2 , resulting in stable PV power close to 2000 kW . The PV voltage is regulated around 550 V , while the current stays near 5000 A . These results confirm that the MPPT ensures maximum PV output, unaffected by load switching events.

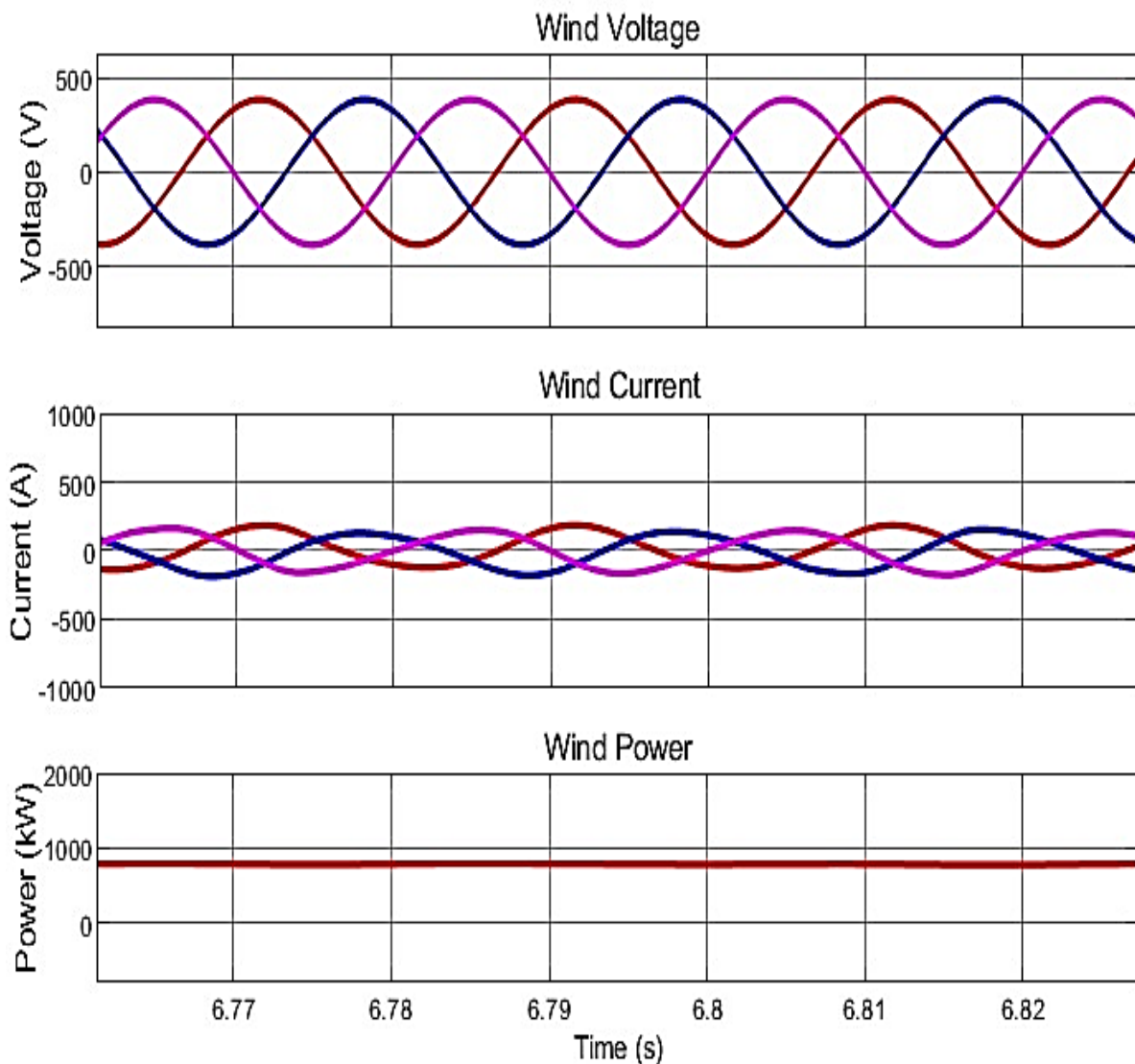


Figure 12. Wind parameters at Mode-2

The wind subsystem in Figure 12 produces 3-phase sinusoidal voltages and currents, with power maintained at approximately 1000 kW . This steady behavior highlights that wind generation remains constant, ensuring a reliable baseline supply regardless of load variations.

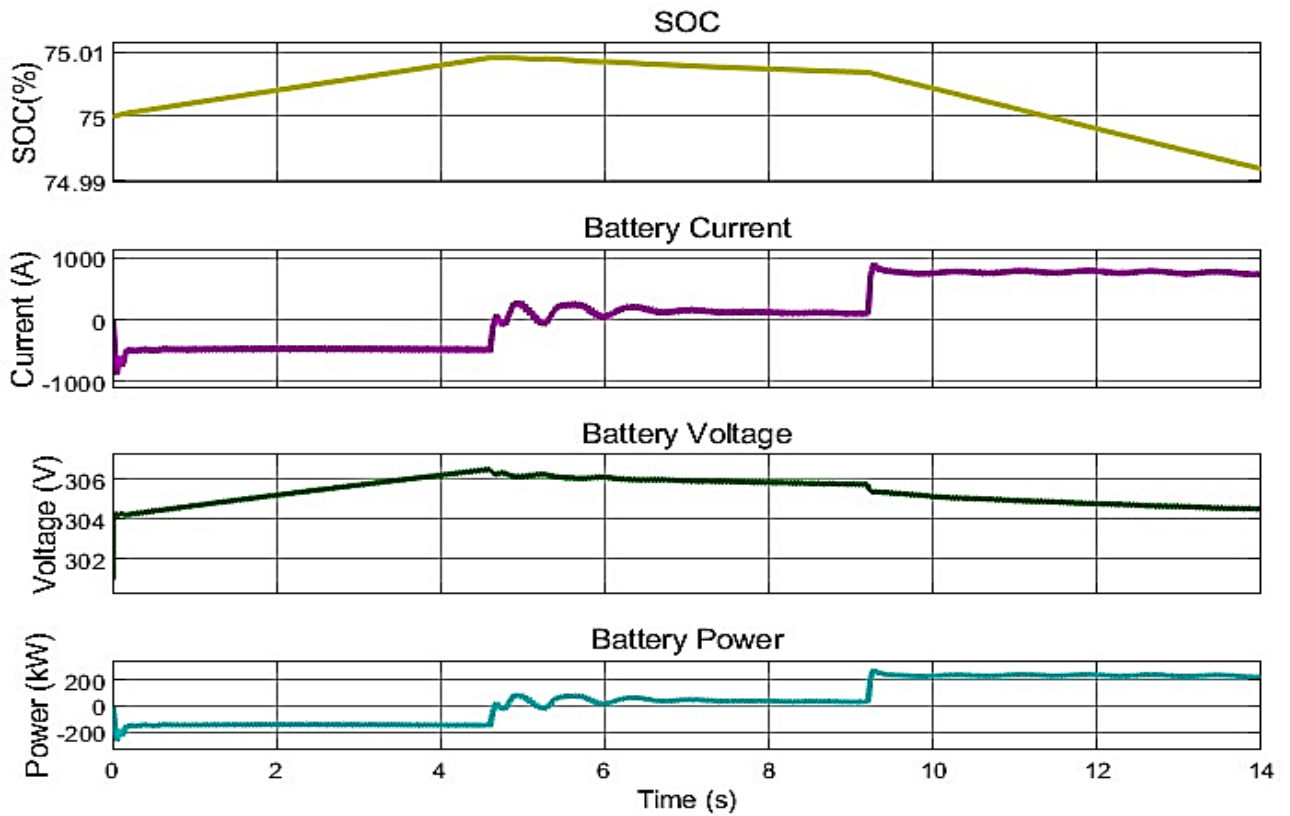


Figure 13. Battery parameters at Mode-2

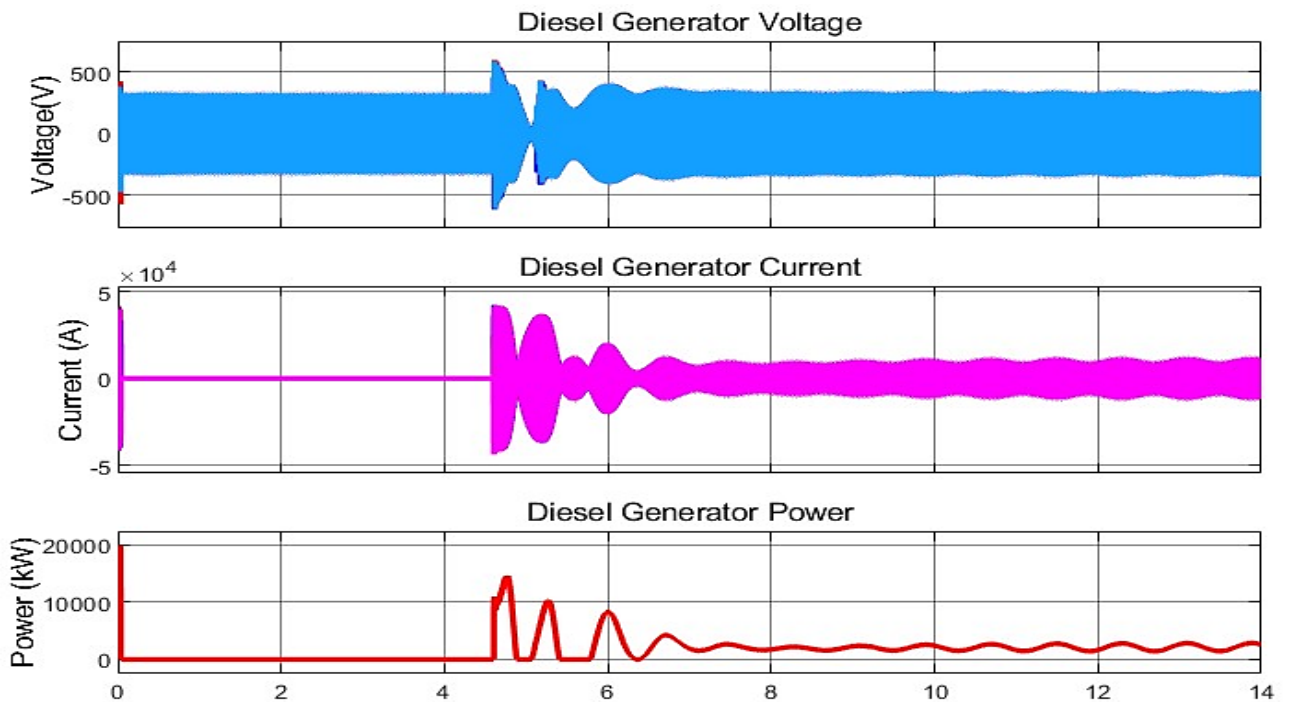


Figure 14. DG parameters at Mode-2

Battery dynamics are shown in Figure 13, where SoC fluctuates slightly between 74.99% and 75%. The current alternates between charging (+1000 A) and discharging (-1000 A) depending on the load. The battery voltage varies from 302 V to 306 V, while the power oscillates between -200 kW and +400 kW, confirming its balancing role in the hybrid system. As depicted in Figure 14 depicts the dynamic response of the diesel generator (DG) during load variations. The revised

manuscript now includes quantitative details explaining the error margins and transient deviations observed in voltage, current, and power. Specifically, the DG voltage fluctuates within $\pm 5\%$ of its nominal value during load transitions, while current exhibits a maximum overshoot of 6% before stabilizing. The power output briefly rises from 1.8 MW to 2.2 MW to compensate for sudden load surges and settles within 1.2 s . These values demonstrate that the system remains well within safe operating limits and confirm the DG's capability to restore equilibrium quickly under varying load conditions.

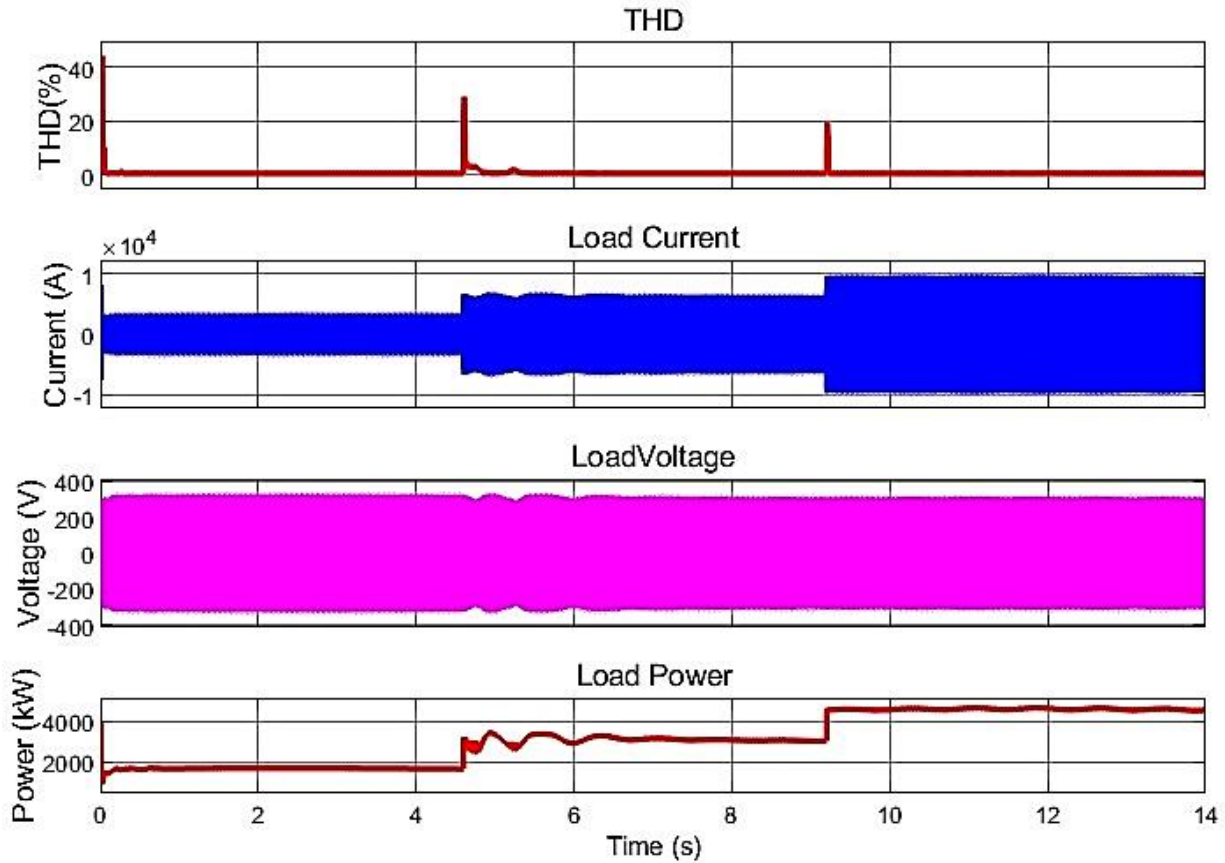


Figure 15. Load parameters at Mode-2

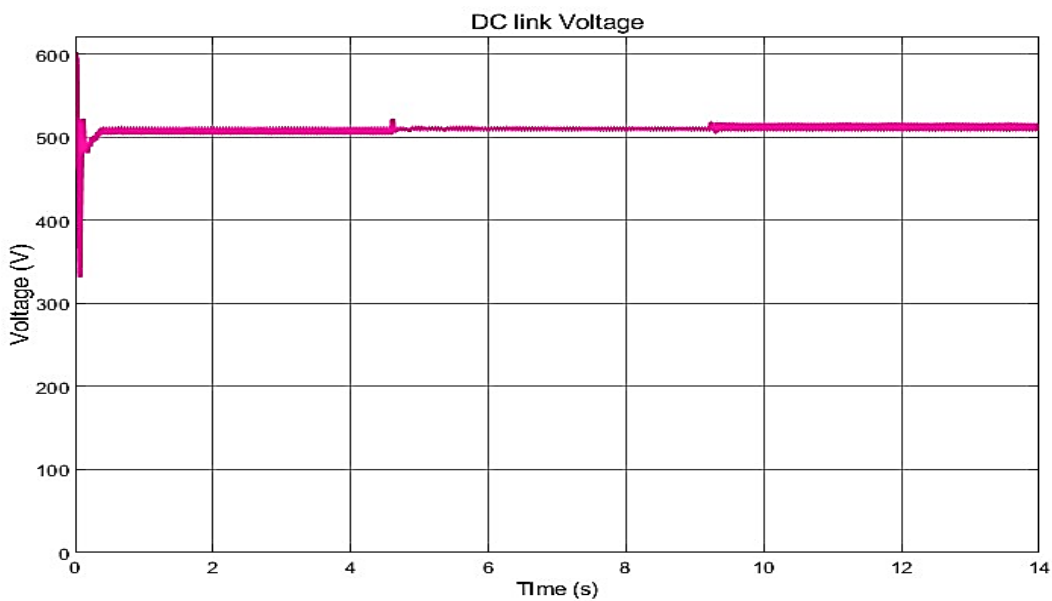


Figure 16. DC link voltage at Mode-2

As illustrated in Figure 15, the load current increases significantly when additional demand is introduced. The load voltage is maintained at about ± 400 V, and the load power rises from 2000 kW to nearly 4000 kW. The THD plot shows short spikes near 20%, but stabilizes close to zero in steady state, confirming acceptable power quality.

The DC link voltage profile in Figure 16 shows regulation around 500 V, with minor deviations during load changes. Quick recovery to the nominal level ensures that inverter operation remains stable and synchronized with the grid. This performance demonstrates the robustness of the control strategy under varying demand.

Table 1. Battery performance parameters under varying irradiance and load conditions

Mode	SoC Range (%)	Voltage Range (V)	Current Range (A)	Power Flow (kW)	Operation
Mode 1 (Varying Irradiance)	74.98 – 75.00	302 – 304	–500 to +1500	–200 to +400	Smooth charge/discharge to stabilize DC link
Mode 2 (Varying Load)	74.99 – 75.00	302 – 306	–1000 to +1000	–200 to +400	Rapid charge/discharge to balance load fluctuations

Table.1 summarizes battery performance under two operating conditions. In Mode 1, minor SoC and voltage variations indicate smooth charge–discharge cycles that stabilize the DC link during irradiance changes. In Mode 2, larger current swings reflect rapid charging and discharging to balance sudden load fluctuations, confirming the battery’s effectiveness in maintaining system stability and power balance

V. CONCLUSION

This work investigated an integrated energy management strategy for a hybrid system consisting of PV, wind, BESS and a DG. The study was carried out in MATLAB/Simulink under two modes of operation: varying irradiance and varying load demand. The proposed EMS effectively coordinated the interaction among different sources to ensure stable operation and reliable supply. In the first mode, the PV system responded dynamically to changes in solar irradiance, while the battery alternated between charging and discharging to smooth fluctuations and support the load. The wind subsystem provided a stable contribution, and the DG acted as a backup source during reduced renewable availability. The system-maintained voltage stability and delivered high-quality power with minimal distortions. In the second mode, where irradiance was held constant and load demand was varied, the EMS regulated source contributions to maintain power balance. The proposed P&O MPPT controller achieved a PV power tracking efficiency of 98.7%, ensuring near-optimal energy extraction under variable irradiance conditions. The battery maintained a stable SoC between 74.98% and 75.00%, with voltage variation confined to 302–306 V and current ranging from –1000 A to +1500 A, demonstrating efficient bidirectional operation and reliable DC-link voltage support during both charging and discharging modes. The load received an uninterrupted and quality supply, while the DC-link voltage remained well regulated. Overall, the proposed EMS demonstrated its ability to maximize renewable energy utilization, reduce dependence on diesel generation, and enhance system efficiency. Despite demonstrating robust energy management and stable operation, the proposed framework has certain limitations. The control model assumes ideal converter efficiency and neglects system losses in interconnecting transformers and cables. Temperature and aging effects on the Li-ion battery are ignored, which may affect long-term SoC accuracy. Furthermore, communication delays and sensor inaccuracies are not considered in the MATLAB/Simulink simulation. Future extensions will incorporate hardware-in-loop testing and economic optimization to validate system feasibility under real-world uncertainties.

References

- [1] Olatomiwa, L., Mekhilef, S., Ismail, M. S., & Moghavvemi, M. (2016). Energy management strategies in hybrid renewable energy systems: A review. *Renewable and Sustainable Energy Reviews*, 62, 821-835.
- [2] Tamoor, M., Tahir, M. A. B., & Zaka, M. A. (2021). Energy management system for integration of different renewable energy system into microgrids. *Int. J.*, 10(2), 1-28.
- [3] Heydari, M., Heydari, A., & Amini, M. (2023). Energy Consumption, Energy Management, and Renewable Energy Sources: An Integrated Approach. *International Journal of Engineering and Applied Sciences*, 9(07), 167-173.
- [4] Vyas, M., Yadav, V. K., Vyas, S., Joshi, R. R., & Tirole, R. (2022). A Review of Algorithms for Control and Optimization for Energy Management of Hybrid Renewable Energy Systems. *Intelligent Renewable Energy Systems*, 131-155.
- [5] Jyoti Saharia, B., Brahma, H., & Sarmah, N. (2018). A review of algorithms for control and optimization for energy management of hybrid renewable energy systems. *Journal of Renewable and Sustainable Energy*, 10(5).
- [6] Aziz, A. S., Tajuddin, M. F. N., Adzman, M. R., Ramli, M. A., & Mekhilef, S. (2019). Energy management and optimization of a PV/diesel/battery hybrid energy system using a combined dispatch strategy. *Sustainability*, 11(3), 683.
- [7] Rekioua, D., Mokrani, Z., Kakouche, K., Rekioua, T., Oubelaid, A., Logerais, P. O., ... & Ghoneim, S. S. (2023). Optimization and intelligent power management control for an autonomous hybrid wind turbine photovoltaic diesel generator with batteries. *Scientific reports*, 13(1), 21830.
- [8] Tazvinga, H., Zhu, B., & Xia, X. (2014). Energy dispatch strategy for a photovoltaic–wind–diesel–battery hybrid power system. *Solar Energy*, 108, 412-420.
- [9] Atieh, A., Charfi, S., & Chaabene, M. (2018). Hybrid PV/batteries bank/diesel generator solar-renewable energy system design, energy management, and economics. In *Advances in Renewable Energies and Power Technologies* (pp. 257-294). Elsevier.
- [10] Jasim, A. M., Jasim, B. H., Baiceanu, F. C., & Neagu, B. C. (2023). Optimized sizing of energy management system for off-grid hybrid solar/wind/battery/biogasifier/diesel microgrid system. *Mathematics*, 11(5), 1248.
- [11] Koussa, D. S., Koussa, M., Rennane, A., Hadji, S., Boufertella, A., Balehouane, A., & Bellarbi, S. (2017). Hybrid diesel-wind system with battery storage operating in standalone mode: control and energy management–experimental investigation. *Energy*, 130, 38-47.
- [12] Thirugnanam, K., Kerk, S. K., Yuen, C., Liu, N., & Zhang, M. (2018). Energy management for renewable microgrid in reducing diesel generators usage with multiple types of battery. *IEEE Transactions on Industrial Electronics*, 65(8), 6772-6786.
- [13] Roumila, Z., Rekioua, D., & Rekioua, T. (2017). Energy management based fuzzy logic controller of hybrid system wind/photovoltaic/diesel with storage battery. *International Journal of Hydrogen Energy*, 42(30), 19525-19535.
- [14] Abbas, A. K., Asal, R. A., Aboud, G. A., Al Mashhadany, Y., & Al Smadi, T. (2024). Optimal Control Strategy for Power Management Control of an Independent Photovoltaic, Wind Turbine, Battery System with Diesel Generator. *International Journal of Electrical and Electronics Research*, 12(3), 1101-1108.
- [15] Urtasun, A., Sanchis, P., Barricarte, D., & Marroyo, L. (2014). Energy management strategy for a battery-diesel stand-alone system with distributed PV generation based on grid frequency modulation. *Renewable Energy*, 66, 325-336.
- [16] Thirunavukkarasu, M., & Sawle, Y. (2021). A comparative study of the optimal sizing and management of off-grid solar/wind/diesel and battery energy systems for remote areas. *Frontiers in Energy Research*, 9, 752043.
- [17] Almihat, M. G. M., & Kahn, M. T. E. (2023). Design and implementation of Hybrid Renewable energy (PV/Wind/Diesel/Battery) Microgrids for rural areas. *Journal of Solar Energy and Sustainable Development*, 12(1).
- [18] Ahmed, F., Al-Abri, R., Yousef, H., & Massoud, A. M. (2024). An optimal energy dispatch management system for hybrid power plants: PV-grid-battery-diesel generator-pumped hydro storage. *IEEE Access*.
- [19] Pranati Katyal, Rajesh Katyal, K.Premkumar, “PV, Wind powered Electric Vehicle Charging Station with Fuzzy and Perturb & Observe MPPT Control”, *Journal of Next Generation Technology (ISSN: 2583-021X)*, 4(3), pp. 1-14. Dec 2024.
- [20] Pranati Katyal, Rajesh Katyal and K.Premkumar, “Energy Management Approaches for Enhanced Performance in Grid-linked Solar PV System with Battery Storage”, *Journal of Next Generation Technology (ISSN: 2583-021X)*, 4(1), pp. 1-16. Jan 2024.

Author's biography



Dr. Pranati Katyal. She got her bachelor's degree in Electrical Engineering from Government College of Engineering, Amaravati, Maharashtra, India in the year 1992. Later she completed her M.Tech (Hons.) in Electrical Engineering from Maulana Azad National Institute of Technology, Bhopal, India in the year 2001. Dr. Pranati Katyal completed her Ph.D., in Electrical Engineering from Anna University, Chennai in the year 2014. She has nearly 30 years of teaching experience. Presently she is working as a Professor in Misrimal Navajee Munoth Jain Engineering college Chennai. Her areas of interest are Power Electronics in Wind and Solar Energy, Electrical Machines and Renewable Energy Sources.



Dr. Rajesh Katyal. He is presently working as Director General in the National Institute of Wind Energy, Chennai under Ministry of New and Renewable Energy, New Delhi. He has completed his BE in Civil Engineering from Nagpur University, Maharashtra. Subsequently, he achieved his M.Tech in Stress and Vibration from Maulana Azad National Institute of Technology, Bhopal, India. Later he was awarded the best Ph.D, award by the Governor of Madhya Pradesh in 2015 under Rajiv Gandhi Technical University, Bhopal Madhya Pradesh, India. He has vast experience in Wind Energy Technology and Offshore Wind farms.



Dr. K. Premkumar currently working as an associate professor in the department of electrical and electronics engineering at Rajalakshmi Engineering College, Rajalakshmi Nagar, Thandalam, Chennai - 602105. Tamil Nadu, India. His current research interests include designing speed and current controllers based on PID controllers, fuzzy logic controllers, ANFIS controllers, and CANFIS controllers for special electrical machines.